ВАК 2024 MODERN ASTRONOMY: FROM THE EARLY UNIVERSE TO EXOPLANETS AND BLACK HOLES
300 years Russian Academy of Sciences

# MHD-Modeling of the molecular filament evolution with numerical FLASH code

I. Sultanov and S. Khaibrakhmanov

Chelyabinsk State University, 129 Br. Kashirinykh, Chelyabinsk, 454001 Russia

**Abstract.** We study numerically the gravitational fragmentation of a cylindrical molecular cloud with large-scale magnetic field. The simulations are performed with the help of the MHD code `FLASH`. We consider two cases: gravitational instability of the filament with initially deformed surface (model of Chandrasekhar and Fermi), and the instability of longitudinal compressible waves (model of Stodolkeiwicz). The simulations under typical parameters show that two types of the cores can be formed as a result of the fragmentation. Gravitational focusing leads to the formation of two massive clumps at the ends of filaments. Those cores move towards the cloud center with supersonic speeds. The instability of initial perturbations results in smaller evenly distributed cores inside the filament. The cores formed due to the instability of compressible waves have almost spherical shapes, while the cores resulted from the fragmentation of the filament with deformed surface are flattened. Typical sizes of the cores of 0.01–0.02 pc are in agreement with observations.

**Keywords:** ISM: clouds, evolution, magnetic fields; magnetohydrodynamics (MHD); methods: numerical

**DOI:** 10.26119/VAK2024.091

# 1 Introduction

Modern observations show that interstellar clouds have a filamentary structure, which is traced from H I super clouds to individual molecular clouds (André et al. 2014). Filaments appear as elongated structures in the emission maps of the interstellar medium. Such filaments can be either cylindrical clouds or gas-dust layers which are seen edge-on (Dudorov & Khaibrakhmanov 2017). Observations show that the typical width of molecular filaments in the regions of star formation is of 0.1 pc, and their length varies from several pc to tens of pc. The temperature in the filaments ranges from 10 K to 25 K, and the gas density ranges from $10^4$ cm$^{-3}$ up to $10^5$ cm$^{-3}$ (Dudorov & Khaibrakhmanov 2017). Polarization mapping revealed the presence of large-scale magnetic fields in filaments. The magnetic field strength increases with the column density and lies in the range from $10^{-5}$ G for low column density clouds with $N = 10^{19}$ cm$^{-2}$ up to $10^{-3}$ G for the dense filaments with $N = 10^{23}$ cm$^{-2}$.

Most protostellar clouds in which star formation occurs are located within filamentary molecular clouds (Konyves et al. 2015). The core formation is associated with the process of gravitational fragmentation (Chandrasekhar & Fermi 1953; Stodólkiewicz 1963; Ostriker 1964). Different regimes of the filament fragmentation are possible depending on its initial state: gravitational collapse at the ends of filament, gravitational fragmentation of the filament with the subsequent formation of evenly distributed cores, and global collapse of the filament towards the center of the cloud (Seifried & Walch 2015). Magnetic field has a great effect on the filament evolution. Almost constant filament width of the order of 0.1 pc can be maintained by magnetic pressure gradient (Dudorov & Khaibrakhmanov 2017). The magnetic field prevents global collapse of the filament towards its axis, so that the collapse becomes possible only at the ends of filament (Sultanov & Khaibrakhmanov 2024).

In this work we perform numerical simulations to study the gravitational fragmentation of the filaments with parallel magnetic field. Based on the simulations, we analyse the properties of molecular cloud cores forming as a result of the fragmentation.

# 2 Model

## 2.1 Perturbations

We consider two models of the gravitational fragmentation. In the first model (Chandrasekhar & Fermi 1953), periodic deformations of the filament surface are introduced. The imcompressible deformations lead to the fragmentation if the wavelength of the deformation exceeds a certain critical value. In the second model (Stodólkiewicz 1963), small compressible waves traveling along the cloud axis are considered. The waves become gravitationally unstable and lead to the cloud fragmentation, if the wavelength exceeds a critical length.

### 2.2 Problem statement

We simulate the gravitational collapse of a cylindrical molecular cloud (filament) with length $H_0 = 2$ pc and radius $r_0 = 0.1$ pc. The molecular weight of the gas is $\mu = 2.31$, temperature $T_0 = 10$ K, adiabatic index $\gamma = 1.001$, concentration $n_0 = 2.6 \times 10^4$ cm$^{-3}$. Mass of the cloud is $10\,M_\odot$. Corresponding free fall time is $t_{\rm ff} = 2 \times 10^5$ years.

We run two simulations: adopting the model of Stodólkiewicz (1963) (STD) and the model of Chandrasekhar & Fermi (1953) (CF). Magnetic field is parallel to the main axis and magnetic field strengths are $10^{-5}$ G and $4.8 \times 10^{-5}$ G respectively for STD and CF runs. Corresponding critical wavelengths are $\lambda_{\rm STD} = 0.244$ pc and $\lambda_{\rm CF} = 1.25$ pc.

In the initial setup, we introduce the small perturbations with $\lambda = 1.19\,\lambda_{\rm STD}$ for run STD and $\lambda = 0.52\,\lambda_{\rm CF}$ for run CF.

### 2.3 Basic equations and solution methods

We study the evolution of the molecular filament using the system of ideal MHD equations. The equations are solved with the help of the numerical code `FLASH 4`, in which the adaptive mesh refinement (AMR) technology is implemented (Fryxell et al. 2018). The equations of ideal MHD are solved using the Godunov-type MUSCL scheme (van Leer 1979). We consider a 3D problem in Cartesian coordinates. The $z$-axis corresponds to the symmetry axis of the filament. The sizes of the computational domain in the $x$-, $y$-, and $z$-directions are $1 \times 1 \times 3$ pc$^3$, and 7 levels of the AMR grid are used. The sizes of the largest cell in the $x$-, $y$-, and $z$-directions are $0.12 \times 0.12 \times 0.12$ pc$^3$, the sizes of the smallest cells are $0.002 \times 0.002 \times 0.002$ pc$^3$, which corresponds to the effective grid resolution of $512 \times 512 \times 1536$ at the 7th AMR level. The Poisson's equation for gravity is solved using the multipole method based on the Barnes–Hut tree (Barnes & Hut 1986).

## 3 Results

In Fig. 1, we plot the gas density distribution and magnetic field lines in the $x$–$z$ plane for run STD at $t = 0$, $1.26\,t_{\rm ff}$ and for run CF at $t = 0$, $1.5\,t_{\rm ff}$. Final moments of time in runs STD and CF correspond to moments, when gravitational collapse of the cores formed at the end of filament starts. In run CF the filament has a stronger initial magnetic field; therefore, its cores form and start to collapse later.

Figure 1 shows that growth of small perturbations leads to filament fragmentation and subsequent formation of cores in both cases. In order to analyse cores properties, we define cores as the densest parts inside the filament.

In run STD nine cores have formed, as indicated in Fig. 1b. Cores 1 and 2 (end cores, hereafter) are the result of the gravitational focusing at the filament's edges, while cores 2–8 (internal cores, hereafter) formed due to the growth of initial perturbations. Internal cores are equidistant from each other at 0.28 pc or 0.96 $\lambda$ approximately and have almost spherical shape. Cores 3–7 have diameter and density of about 0.006 pc and $7 \times 10^6$ cm$^{-3}$, while cores 2 and 8, located close to the ends, are larger and more massive, of around 0.002 pc and $3.2 \times 10^9$ cm$^{-3}$. End cores are flattened along the magnetic field direction and have sizes of $0.0038 \times 0.002$ pc. Cores 1, 9 and 2, 8 are moving towards the cloud center with supersonic velocities of approximately 3 km/s.

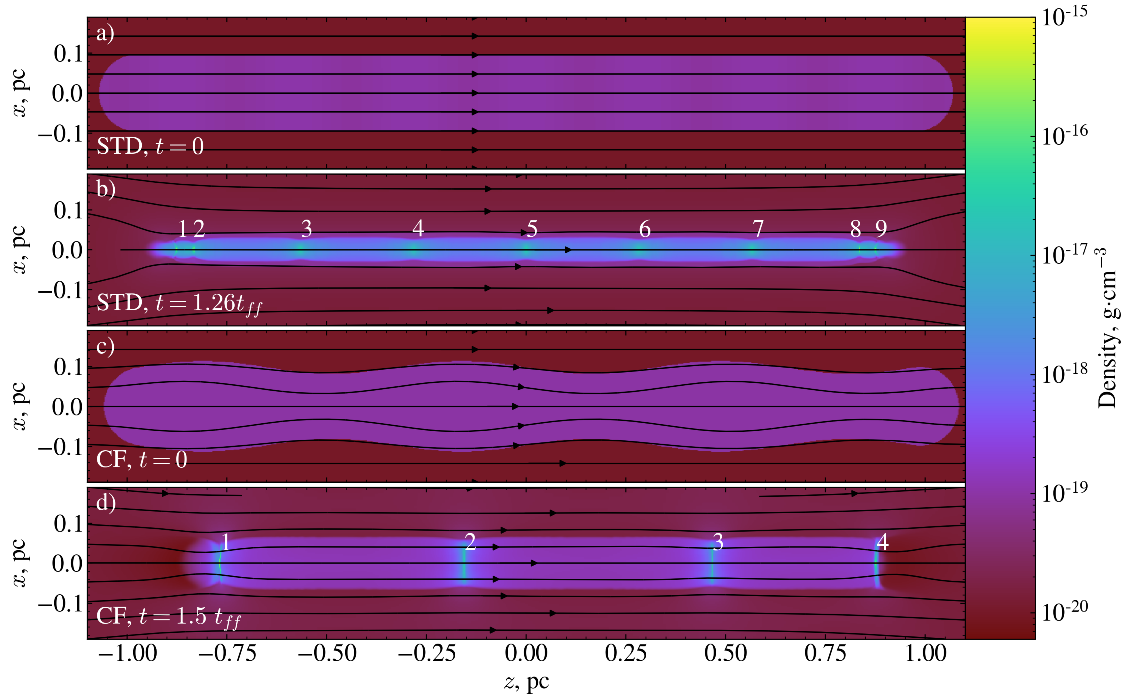


**Fig. 1.** The distribution of gas density (color map) and magnetic field lines (black lines with arrows) in the $x$–$z$-plane for two considered cases. Panels (a) and (b): run STD at $t = 0$ and $t = 1.25\,t_{\rm ff}$, respectively. Panels (c) and (d): run CF at $t = 0$ and $t = 1.5\,t_{\rm ff}$ respectively.

In run CF, four cores have formed. Distance between cores 1, 2 and 3 is about 0.614 pc or 0.94 $\lambda$. These cores are formed due to the gravitational instability of initial surface deformations, and have similar properties. The shape of the core 1 is closer to the spherical one, because of additional effect of gravitational focusing at the end of filament. This core has flattened envelope. Cores 2–4 are flattened along magnetic field, and have typical sizes of $0.013 \times 0.002$ pc (cores 2 and 3) and $0.004 \times 0.002$ pc (core 4). Cores density varies in the range from $10^7$ cm$^{-3}$ in the filament center up to $10^8$ cm$^{-3}$ at its ends. Cores 1 and 4 are moving towards the cloud center with supersonic velocities of 4 km/s and 2 km/s.

## 4 Summary

Our simulations have shown that the different kinds of the initial perturbations in the molecular filaments lead to different properties of the cores formed as a result of the fragmentation. Gravitational instability of compressible waves results in larger cores as compared to the case of the filament with deformed surface. In the former case, the cores are more spherical, while in the latter case the cores has flattened shape. Typical maximum sizes of the cores formed in the case of initially deformed filament are 0.01 pc, which is in agreement with values obtained from observations for the TMC1 region in the Taurus Molecular Cloud (Kirk et al. 2024).

**Acknowledgements.** The simulations were carried out using the computational cluster of the Chelyabinsk State University.

## Funding

The work is financially supported by the Russian Science Foundation (No. 24-22-20041).

## References

André P., Di Francesco J., Ward-Thompson D., et al., 2014, Protostars and Planets VI, ed. Beuther H., Klessen R.S., Dullemond C.P., Henning T., p. 27
Barnes J. and Hut P., 1986, Nature, 326, 6096, p. 446
Chandrasekhar S. and Fermi E., 1953, Astrophysical journal, 118, p. 116
Dudorov A.E. and Khaibrakhmanov S.A., 2017, Open Astronomy, 26, 1, p. 285
Fryxell B., Olson K., Ricker P., et al., 2000, Astrophysical Journal Supplement, 131, 1, p. 273
Kirk J.M., Ward-Thompson D., Di Francesco J., et al., 2024, Monthly Notices of the Royal Astronomical Society, 532, 4, p. 4661
Konyves V., André Ph., Men'shchikov A., et al., 2015, Astronomy & Astrophysics, 584, id. A91
van Leer B., 1979, Journal of Computational Physics, 32, 1, p. 101
Ostriker J., 1964, Astrophysical Journal, 140, p. 1056
Seifried D. and Walch S., 2015, Monthly Notices of the Royal Astronomical Society, 452, 3, p. 2410
Stodólkiewicz J.S, 1963, Acta Astronomica, 13, p. 30
Sultanov I.M. and Khaibrakhmanov S.A., 2024, Astronomy Reports, 68, 1, p. 60